

¹Cold-Formed Steel U-Section Encased in Simple Support Reinforced Concrete Beam.

Ahmed Youssef Kamal^{*1}, Nader Nabih Khalil^{1a}

¹Benha Faculty of Engineering, Benha University, Egypt.

Abstract. Cold-formed steel sections are widely used in construction work as its low cost. This paper presents a series of bending tests, to examine the influence of encasing cold-formed steel (U-section) in a reinforced concrete beam on the beams capacities, mode of failure and ductility. The cold-formed steel section breadth, height, and length are the main parameters studied and presented. Eight full-scale encased composite beams have tested under lateral loading up to failure, in addition, to one full-scale reinforced concrete beam (without cold-formed steel sections). The experimental results have recorded and monitored to clarify the influence of the studied parameters on the composite beam behavior. The experimental results have compared with the reference beam. It has found that the cold-formed steel (U-section) increased the beam load carrying capacity and improved the beam ductility. It has observed that encasing the formed steel sections reduced the influence of the steel sections local buckling.

Keywords: Encased; Beam; U-section; Cold-formed Sections.

* Corresponding author, Assistant Professor, E-mail: aykmar@yahoo.com

1. Introduction

Steel-concrete composite structure element has been widely used in high-rise building construction, in order to increase the strength and the ductility of the structural elements. The advantages of the steel and concrete material are included in the steel-concrete composite structures. Composite steel-concrete are classified in three figures or shapes, the first one is section compose of concrete slab rest on steel section, encased steel section in concrete and filled tube steel section with concrete. Composite beams can carry various forms; one of these forms is consisting of cold-formed steel section encased in concrete. Qiyin et al. [1] have reported that the steel-encased concrete composite beams and steel-reinforced composite beams both have the shortcoming, that the former slip is too big.

Cold-formed steel cross-sections have used in primary structural elements, as well as secondary load-carrying members. L.Fiorino et al. [2] have used CFS as framing systems in multi-storey buildings. J.B.P.Lim et al. [3] have used CFS as portal frame in single-story industrial building with intermediate and short span. Reasonable force, lighter weight, eases manufacturing, transportation, and erection, are the most popular advantages of the cold-formed steel cross-sections. Wang H. et al. [4] have figured out that cold-formed steel sections (CFS), could be effortlessly formed and sized to fit specific design requirements, as they are manufactured from steel sheets have a nominal thickness between 0.8 and 3 mm, and can be formed into many shapes (open sections, channel sections, Z-sections, etc.) by cold-rolling technique.

Due to the neglected (CFS) thickness to width dimension, (CFS) sections are mainly exposed to global and distortional buckling modes. Cold-formed steel (CFS) sections has no advantages to resist bending load alone, therefore it is not suitable for the flexural member, local buckling was early predicted in cold-formed sections subjected to compression or shear stresses. Therefore, the buckling of the cold-formed steel sections under compression or shear may take place before the overall member buckling or overall member failure by yielding or lateral buckling, this phenomenon called local buckling. Thus, local buckling imposes a limit to the extent use of thin-walled sections.

Dinis et al. [5] found out that the flange local buckling and the distortional buckling are the main factors governing the failure modes of cold-formed steel sections (CFS), arising from in-plane bending moments. Pham et al. [6] have reported that improving the flange or web local buckling performance can be achieved by providing a vertical longitudinal stiffener in the direction of the longitudinal stresses. Wang et al. [7] have said that by plate mechanics, the edge stiffeners (channel flange, and intermediate stiffeners in the flange or web) can enhance the strength of the cold-formed steel (CFS) sections by supporting the flat plate elements of sections out-of-plane. Ammar et al. [8] have proved that good flexure performance and beam ductility recorded by increasing the steel percentage in the encased beam. L. Krishnan et al. [9] have used the triangular corrugation web to increases the cold-formed steel (CFS) sections flexural capacity.

J. Lee et al. [10] have optimized the (CFS) elements by changing the dimensions of cross-sections, while W.Ma et al. [11] have optimized the (CFS) elements by using Genetic Algorithms according to EC3 [12]. J.Z. Leng et al. [13] have optimized the (CFS) elements by incorporating some end-user constraints and have limited the manufacturing process to a certain numbers of rolling.

This paper presents a method to improve local buckling of cold-formed steel sections (CFS) by encasing the (CFS) sections in concrete section, to improve both local buckling performance and

beam flexural capacity. The present study monitoring and study the effect of cold-formed steel (CFS) section breadth, height, and length on the composite beam flexural capacity and ductility. In addition to that, the modes of failure of the encased composite beam have studied.

2. Experimental investigation

2.1. Material Properties

Nine specimens were fabricated and tested in the concrete laboratory of Benha faculty of engineering, Egypt. One of them was concrete beam reinforced by top and bottom steel bars without cold-formed steel sections and referred as a reference beam. The other specimens were enhanced by encased cold-formed U-steel section; with the same reference beam concrete dimensions and reinforcement.

All dimensions measurements and material properties were accurately taken into account, Figs. 1(a)-(c) show a description of the specimen dimension and reinforcement. All specimens were simply supported with total length of 1500 mm, and net length (space between supports) of 1400 mm, the cross section molded as square shape with side-length of 150 mm. All beams were longitudinally reinforced with two top and bottom steel bars with diameter of 12 mm (as a tension and compression reinforcement), reflect a reinforcement ratio of 0.02.

Tension tests of three standard samples were taken from the longitudinal bars, the test results produced average yield strength of 37 kg/mm^2 , and an average elastic modulus of 20900 kg/mm^2 . All beams were also transversely reinforced by closed stirrups resisting shear with diameter of 8 mm, spaced at 200 mm center to center along the beam length; it also makes a good engagement to the longitudinal bars and enhances the beam ductility, as shown in Fig. 1(b).

The transverse reinforcements were with average yield strength of 24 kg/mm^2 , and the average elastic modulus was 20000 kg/mm^2 . Wooden molds manufactured with internal dimensions of $(150 \text{ mm} \times 150 \text{ mm} \times 1500 \text{ mm})$ were used in casting the specimens. The molds were stiffened enough to prevent any significant movement during concrete pouring. A concrete cover of 10 mm was provided for the reinforcements at top, bottom, and sides, as shown in Fig. 1(c).

Tension test of three standard samples were taken from cold-formed steel sections. The elastic modulus and yield stress were recorded. The cold-formed steel U-Section was with constant thickness of 2 mm, average yield strength of 28 kg/mm^2 , and an average elastic modulus of 19800 kg/mm^2 . The centroids of both the (CFS) section and the geometric center of the concrete beam cross section were coincident, as shown in Fig. 1(c).

Three standard concrete cubes with 150 mm side length, were taken from the concrete pouring and crushed in a standard concrete compression test. The average concrete compressive strength for the three cubes (at testing time) was 3.1 kg/mm^2 , as results of laboratory test with average concrete volume weight of 2300 kg/m^3 .

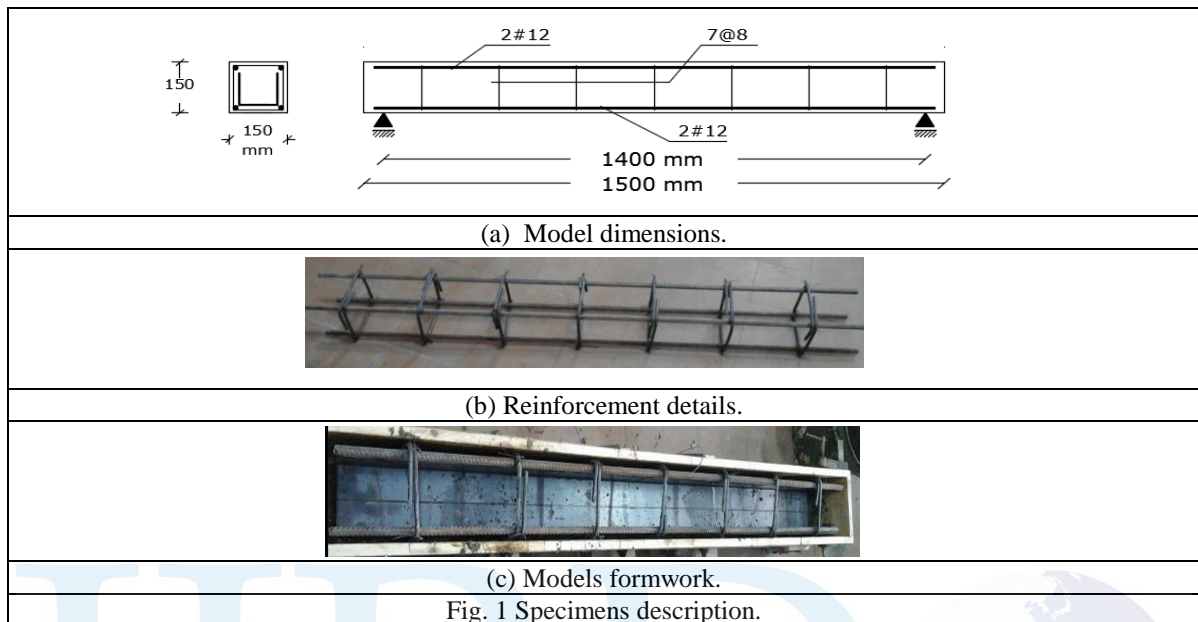


Table 1, shows the details of the experimental program, to evaluate and monitoring the studied parameters affect the structural behavior of the encased beams using cold-formed steel U-section. The experimental program consisted of three groups; to study the effect of different cold-formed steel U-section factors such as; the cold-formed steel U-section width, height, and length.

Table 1 Specimens details.

Specimens	h_s (mm)	b_s (mm)	L_s (mm)	ψ	η	λ
CFS1-1	95	110	1450	0.73	0.63	1.0
CFS2-1	95	75	1450	0.5	0.63	1.0
CFS3-1	95	50	1450	0.33	0.63	1.0
CFS1-2	---	110	1450	0.73	0	1.0
CFS2-2	50	110	1450	0.73	0.33	1.0
CFS3-2	70	110	1450	0.73	0.47	1.0
CFS4-2	95	110	1450	0.73	0.63	1.0
CFS1-3	95	110	1450	0.73	0.63	1
CFS2-3	95	110	930	0.73	0.63	0.66
CFS3-3	95	110	460	0.73	0.63	0.33

* Reference beam with concrete square cross section (150*150 mm), total length of 1500 mm, with top and bottom reinforcement of 2#12 mm.

** CFS (specimen number)-(group number).

*** b: is the concrete beam width,

b_s : is the cold-formed steel section width. (ψ): is the normalized width ($\psi = b_s/b$).

h_s : is the cold-formed steel section height.

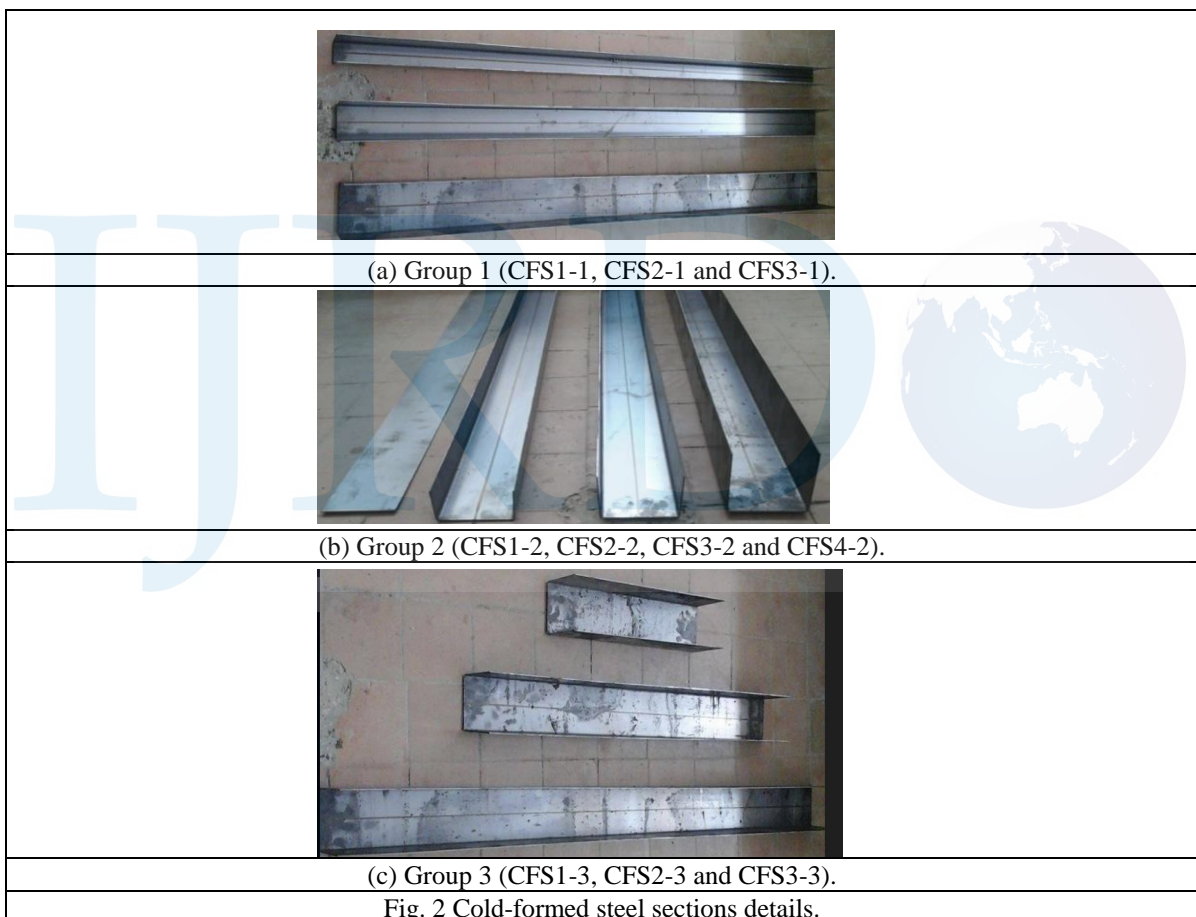
h: is the concrete section height. (η): is the normalized height ($\eta = h_s/h$).

L: is the concrete beam net length.

L_s : is the cold-formed steel section length. (λ): is the normalized length ($\lambda = L_s/L$).

First group considered the cold-formed steel U-section width, and consists of three beams (CFS1-1, CFS2-1, and CFS3-1) with different variable normalized width (ψ) of (0.73, 0.5 and 0.33) respectively. The second group considered the cold-formed steel U-section height, consists of four beams (CFS1-2, CFS2-2, CFS3-2 and CFS4-2) with variable normalized height (η) of (0.0, 0.33, 0.47 and 0.63) respectively. While the third one considered the cold-formed steel U-section length, consists of three beams (CFS1-3, CFS2-3, and CFS3-3) with variable normalized length (λ) of (1.0, 0.66 and 0.33) respectively.

Fig. 2 shows the cold-formed steel section details, which encased in concrete beam with the same reference beam details and dimensions.



2.2. Test setup

All specimens were simply supported and loaded with mid-span concentrated load. The load was recorded by digital load cell connected to a hydraulic jack. While vertical displacements were measured by Linear Variable Differential Transformer (LVDT's) with magnetic base, distributed along the specimen length, two in the left side of the specimen (LVDT 1,2), one under the concentrated load (LVDT 3) and one at mid-span between the applied concentrated load and the right support (LVDT 4), as shown in Fig. 3.

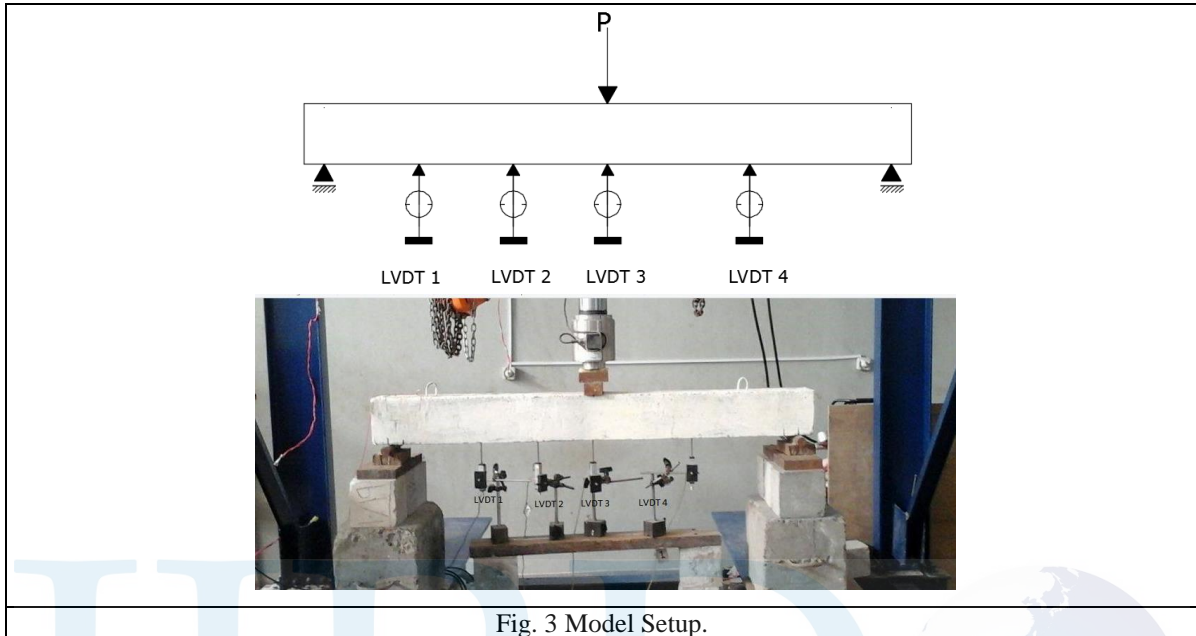


Fig. 3 Model Setup.

Before concrete pouring, electrical resistance strain gauge with length of 10 mm (120 ohm) resistance was glued at the bottom of the cold-formed steel section mid-span, to measure the steel longitudinal strain. The strain gauge was covered by special material for water proofing, as shown in Fig. 4. All results (load, deflections, and strain) were automatically recorded by a computer system and saved as Excel file.

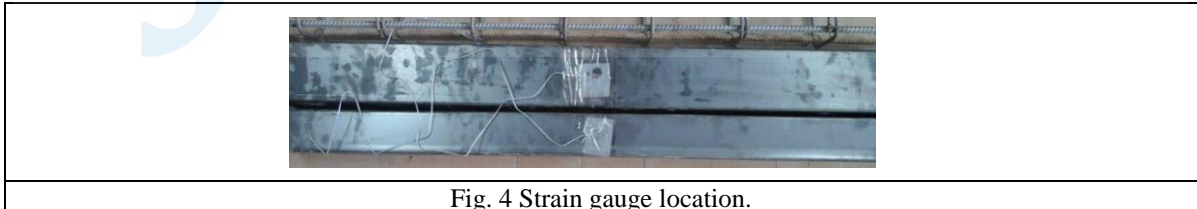


Fig. 4 Strain gauge location.

3. Results and discussions

3.1. Cracking and failure load.

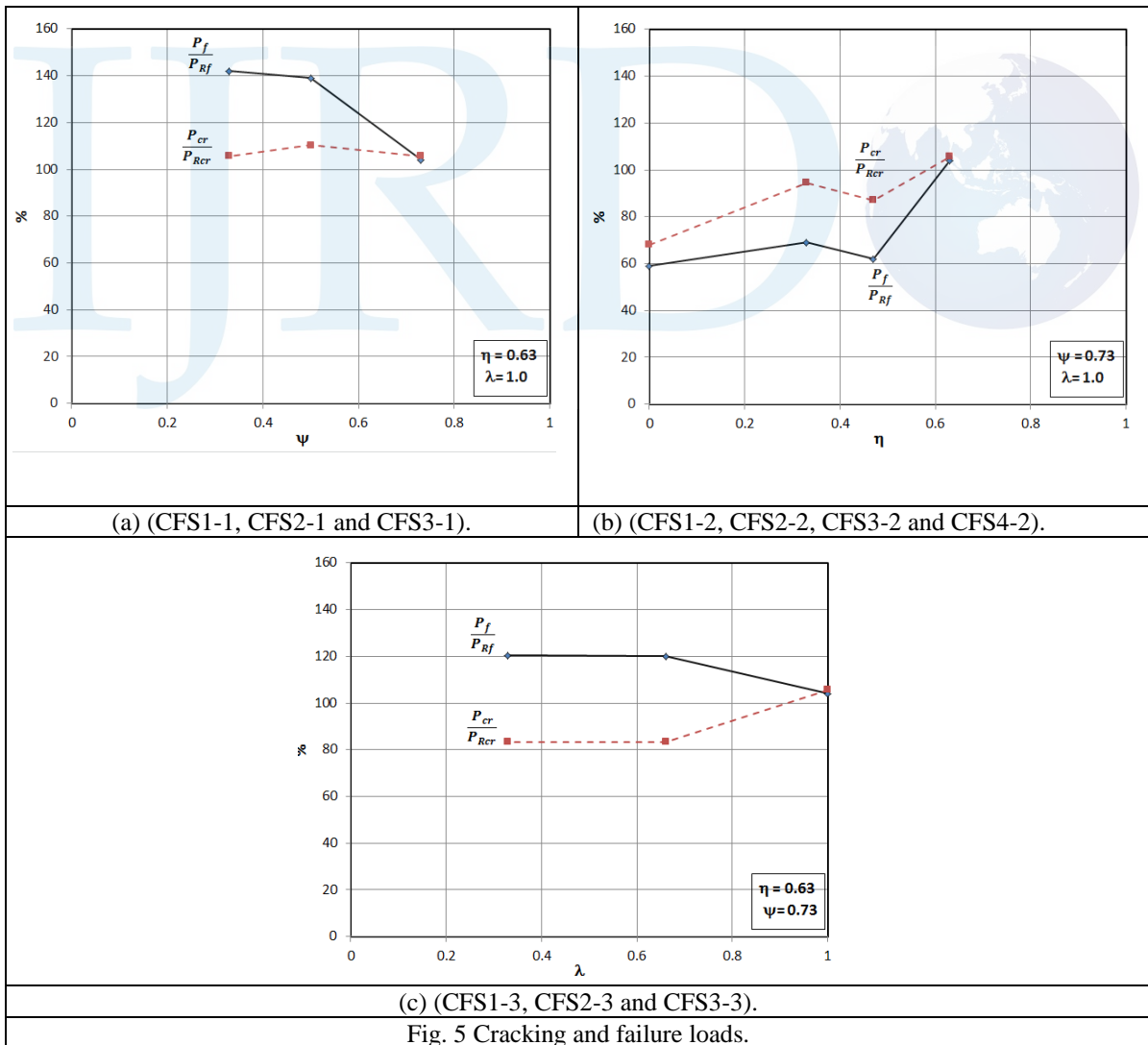
The reference beam failed in ductile flexure mode, with a maximum load capacity of 4110 kg, and cracking load of 2700 kg, Table 2.

Providing the cold-formed steel (CFS) U-Section with different values of normalized width (ψ), for specimens (CFS2-1 and CFS3-1) increase the beam load capacity with a noticeable value of (39 and 42 % respectively) compared with that of reference beam. While specimen (CFS1-1) increase the beam load capacity by only 4 % with respect to reference beam. Cold-formed steel section in models (CFS1-1, CFS2-1 and CFS3-1) delayed the appearance of concrete cracks by (6,

10 and 6 %) respectively, with respect to reference beam, as shown in Fig. 5(a), (which represents the cracking and failure loads as a percentage of that of reference beam).

Models (CFS1-2, CFS2-2 and CFS3-2) fail with decreasing in the load capacity by (41, 31 and 38 %) respectively, with respect to the reference beam. While model (CFS4-2) fails with a little increase of 4% in the beam load capacity, with respect to the reference beam, as shown in Fig. 5(b). As Models (CFS1-2, CFS2-2 and CFS3-2) fail early than reference beam, the concrete cracks for those models were appeared early by (32, 6 and 13 %) than the reference beam, as shown in Fig. 5(b).

Decreasing the cold-formed steel (CFS) length forced the models (CFS2-3 and CFS3-3) to fail, with increasing in the beam load capacity by (20 %) for both, with respect to that of reference beam, as shown in Fig. 5(c). While model (CFS1-3) with (CFS) full-length, fails with increasing in the load capacity by (4 %) with respect to the reference beam, as shown in Fig. 5(c). The concrete cracks appeared early by 17 % than that of reference beam, for models (CFS2-3 and CFS3-3).



Cracking factor (F_{cr}), was defined as the percentage of the cracking load to the failure load, to declare the relationship between the cracking and failure load, the cracking load for the reference beam was 66 %. For the first group this factor was the same for model (CFS1-1), and reduced to (52, 49 %) for models (CFS2-1, CFS3-1) respectively, as shown in Fig. 6(a). The cracking factor increased for the second group to (76, 90 and 92 %) for models (CFS1-2, CFS2-2 and CFS3-2) respectively, as shown in Fig. 6(b). The cracking factor decreased for the third group to (46, 45 %) for models (CFS2-3, CFS3-3) respectively, as shown in Fig. 6(c).

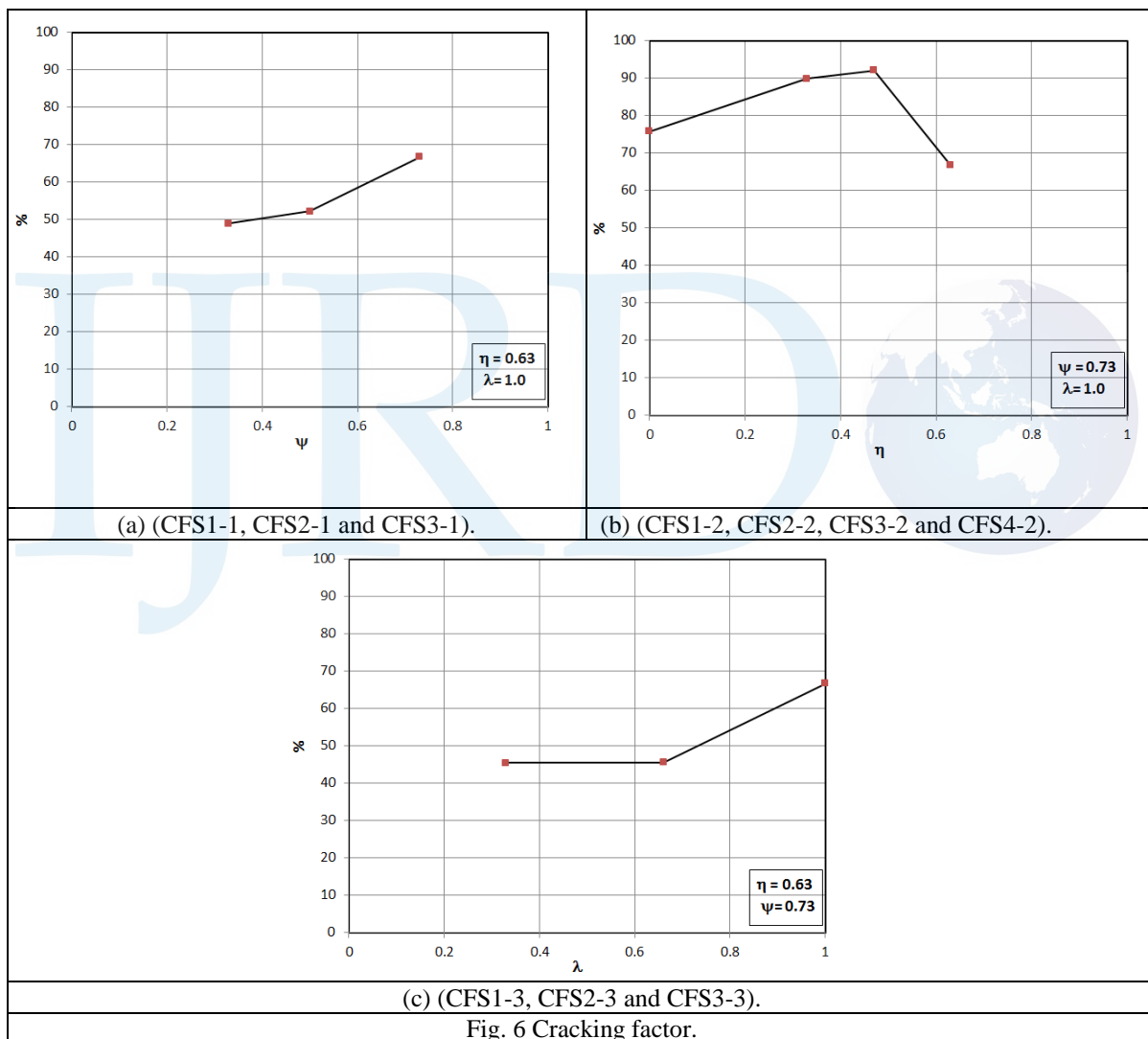


Fig. 6 Cracking factor.

Table 2 Specimens failure mode.

Group	Specimen	P_{cr} (kg)	P_f (kg)	F_{cr} %	Mode of failure
1	CFS1-1	2855	4275	67	Local buckling
	CFS2-1	2980	5713	52	Local buckling / Shear
	CFS3-1	2855	5837	49	Flexural / Shear
2	CFS1-2	1840	2425	76	Flexural / Splitting
	CFS2-2	2550	2836	90	Flexural / Shear
	CFS3-2	2350	2550	92	Local buckling
	CFS4-2	2855	4275	67	Local buckling
3	CFS1-3	2855	4275	67	Local buckling
	CFS2-3	2250	4930	46	Flexural / Shear
	CFS3-3	2250	4950	45	Flexural / Shear
Reference beam		2700	4110	66	Flexural

P_{cr} : Cracking load.
 P_u : Failure load.
 F_{cr} : Cracking factor.
 P_{Rcr} : Reference Cracking load.
 P_{fu} : Reference Failure load.

3.2. Failure mode.

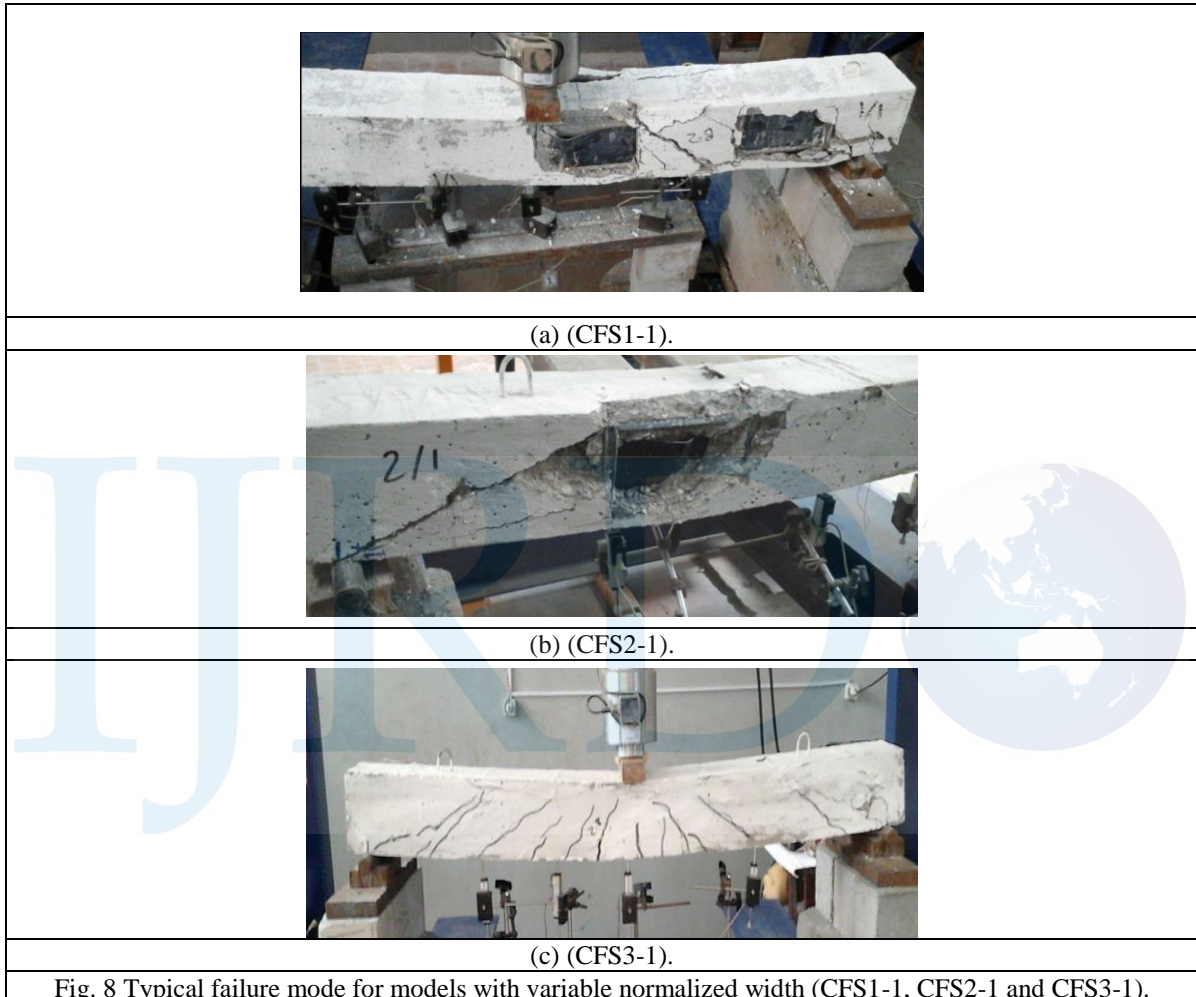
Fig. 7 shows the crack pattern of the reference beam, the reference beam failed in ductile flexure mode. The crack pattern of the reference beam shows flexural cracks for both sides distributed along the reference beam length. The flexural cracks started at the beam bottom mid-span, and propagated toward the concentrated load until beam failed.



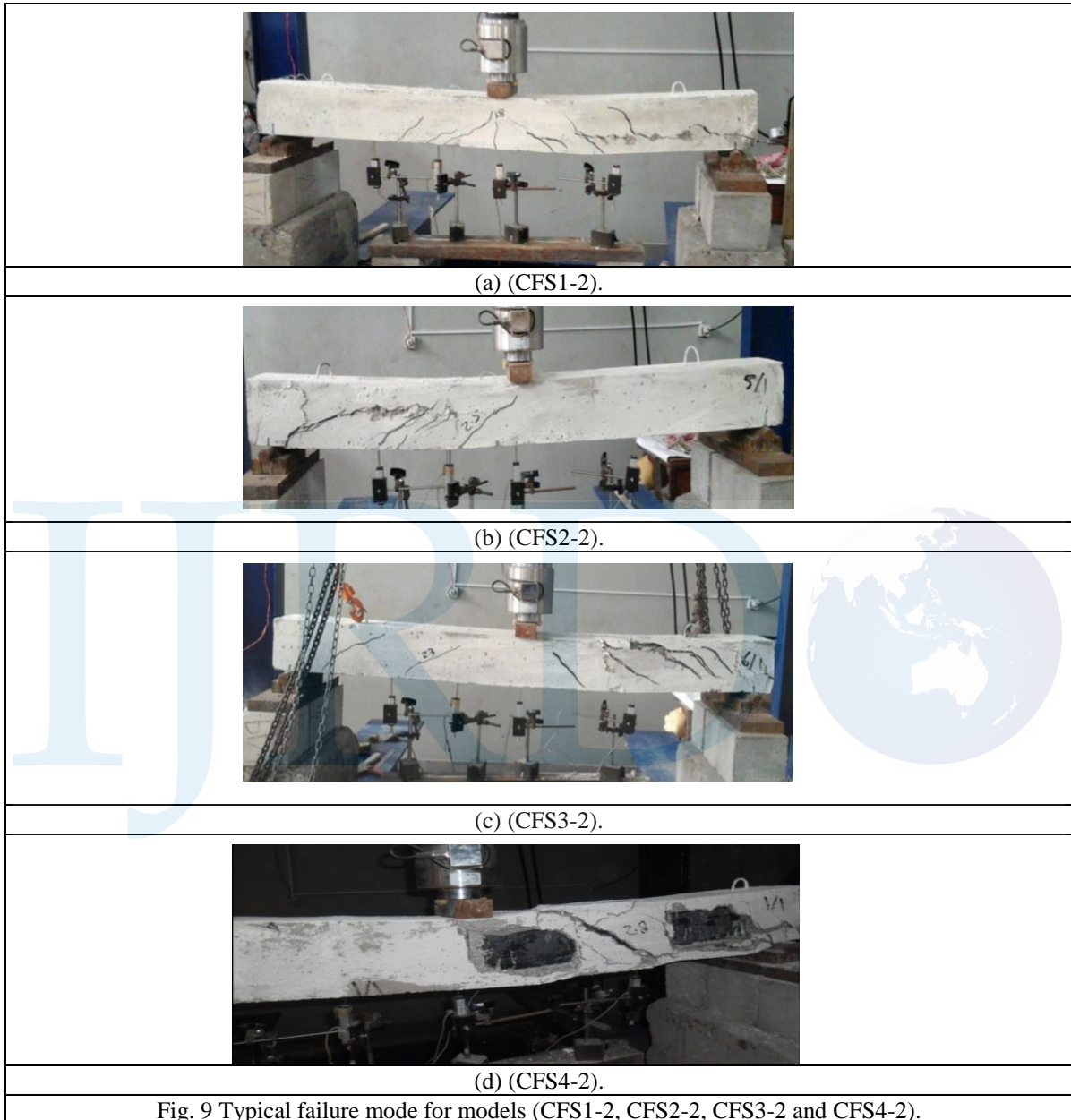
Fig. 7 Typical reference beam failure mode.

Cold-formed steel section in models (CFS1-1 and CFS2-1) with a normalized width ($\psi=0.73, 0.5$) changes the failure mode to concrete side crushing due to local buckling occurred in the (CFS) web as a result of relatively small concrete cover resist the (CFS) web local buckling, ended by shear failure in model (CFS2-1), as shown in Figs. 8(a)-(b). While flexure failure mode was observed in model (CFS3-1) with a normalized width ($\psi=0.33$), ended by shear failure, relative thick concrete cover contributed in preventing the local buckling which led to increase the model load capacity by 42 % and achieve good benefits of (CFS) existence, as shown in Fig. 8(c).

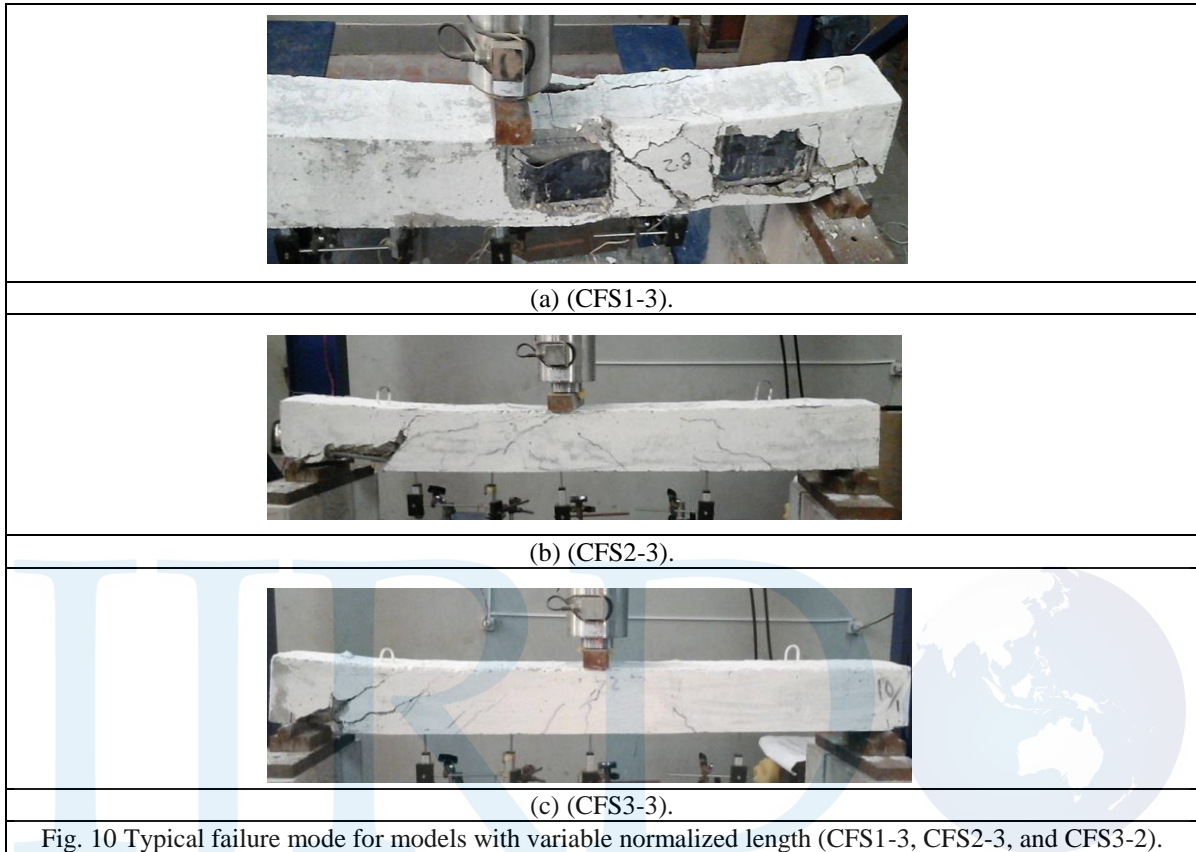
Increasing by 30 % (in average) in the cold-formed mid-span strain for model (CFS3-1), with respect to that for model (CFS2-1) was observed which indicates a stress concentration.



For model (CFS1-2) with no web ($\eta=0$), the failure mode was flexural mode combined with shear splitting failure; the cracking pattern started with mid-span flexural cracks, propagated toward the concentrated load combined with shear splitting cracks, as shown in Fig. 9(a). Model (CFS2-2) fails with flexure failure ended by sudden shear failure, as shown in Fig. 9(b). Models (CFS3-2 and CFS4-2) fail with cold-formed steel section web local buckling, as shown in Figs. 9(c)-(d). Increasing by 35 % (in average) in the cold-formed mid-span strain for a model (CFS1-2) with no web compared with that for model (CFS3-2) was observed.



Decreasing the cold-formed steel (CFS) length force the models (CFS2-3 and CFS3-3) to fail with initiation of flexure cracks ended with sudden shear failure, as shown in Figs. 10(b)-(c). While model (CFS1-3) with (CFS) full-length fail with cold-formed steel section web local buckling, as shown in Fig. 10(a). Increasing by 25 % (in average) in the cold-formed steel mid-span strain for a model with (CFS3-3), compared with that for model (CFS2-3) was observed.



3.3. Deflections

By the Linear Variable Differential Transformer (LVDT's) records the deflected shapes for specimens (CFS1-1, CFS2-1 and CFS3-1) were plotted along the beam length at the same load level (linear stage), and were compared with the reference beam, as shown in Fig. 11. The figure shows that with increasing in the normalized width (ψ), there was a decrease in the beam deflections by (17, 13, 9 %) in average for specimens (CFS1-1, CFS2-1 and CFS3-1) respectively, with respect to that of reference beam.

In addition, the deflected shape for specimens (CFS1-3, CFS2-3 and CFS3-3) were plotted along the beam length at the same load level (linear stage), and was compared with the reference beam, as shown in Fig. 12. The figure shows that there was a decrease of (17, 4 % in average), in the beam deflection for specimens (CFS1-3 and CFS2-3) respectively, with respect to that of reference beam. While specimen (CFS3-3) increase the deflections by (6 % in average) compared with that of reference beam, from that the cold-formed steel section with full length share in decreasing the deflection more than that with less length.

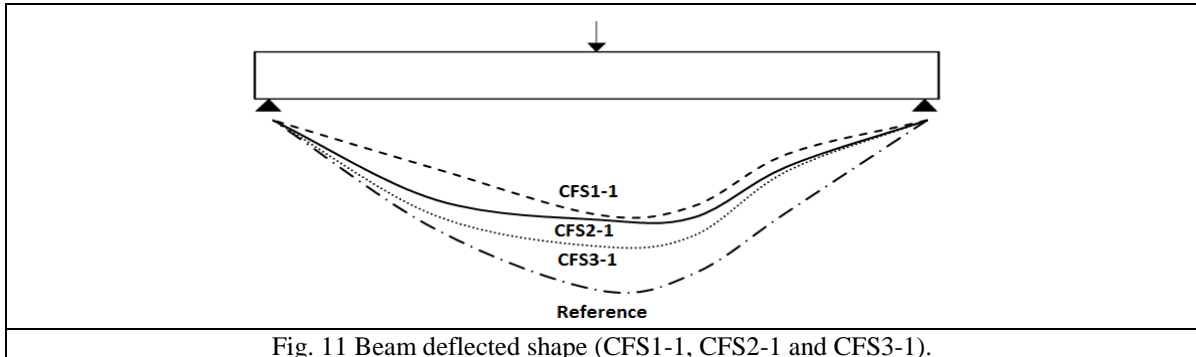


Fig. 11 Beam deflected shape (CFS1-1, CFS2-1 and CFS3-1).

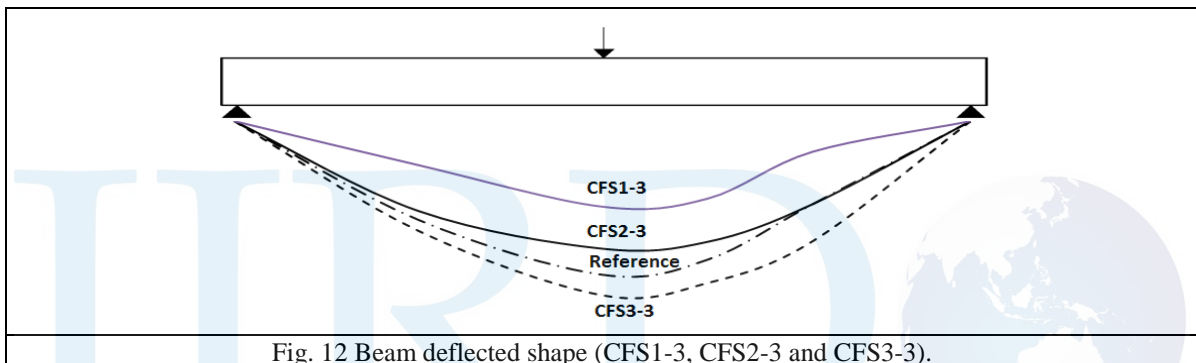
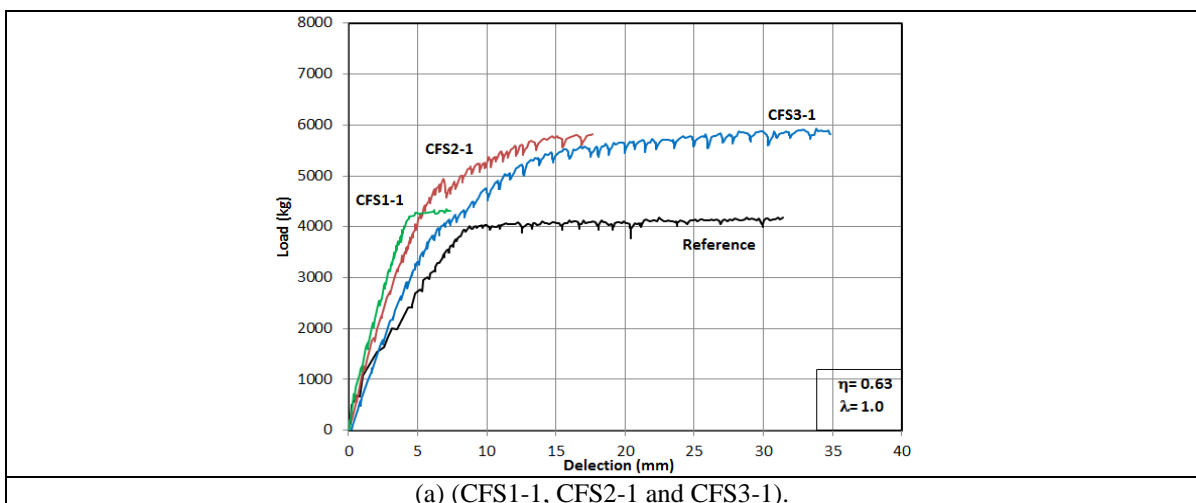


Fig. 12 Beam deflected shape (CFS1-3, CFS2-3 and CFS3-3).

The load-deflection curves for models (CFS2-1, CFS2-2, CFS3-2 and CFS4-2) at the specimen mid-span, illustrates the semi-ductile (local buckling) failure for these specimens, as shown in Fig. 13. While the load-deflection curve for model (CFS3-1) at the specimen mid-span, illustrates the ductile (flexure) failure for this model, as shown in Fig. 13.

The deflection-load curves at the mid-span specimen (CFS2-3 and CFS3-3) reflect the brittle failures (shear failure) for those specimens, as shown in Fig. 13.



(a) (CFS1-1, CFS2-1 and CFS3-1).

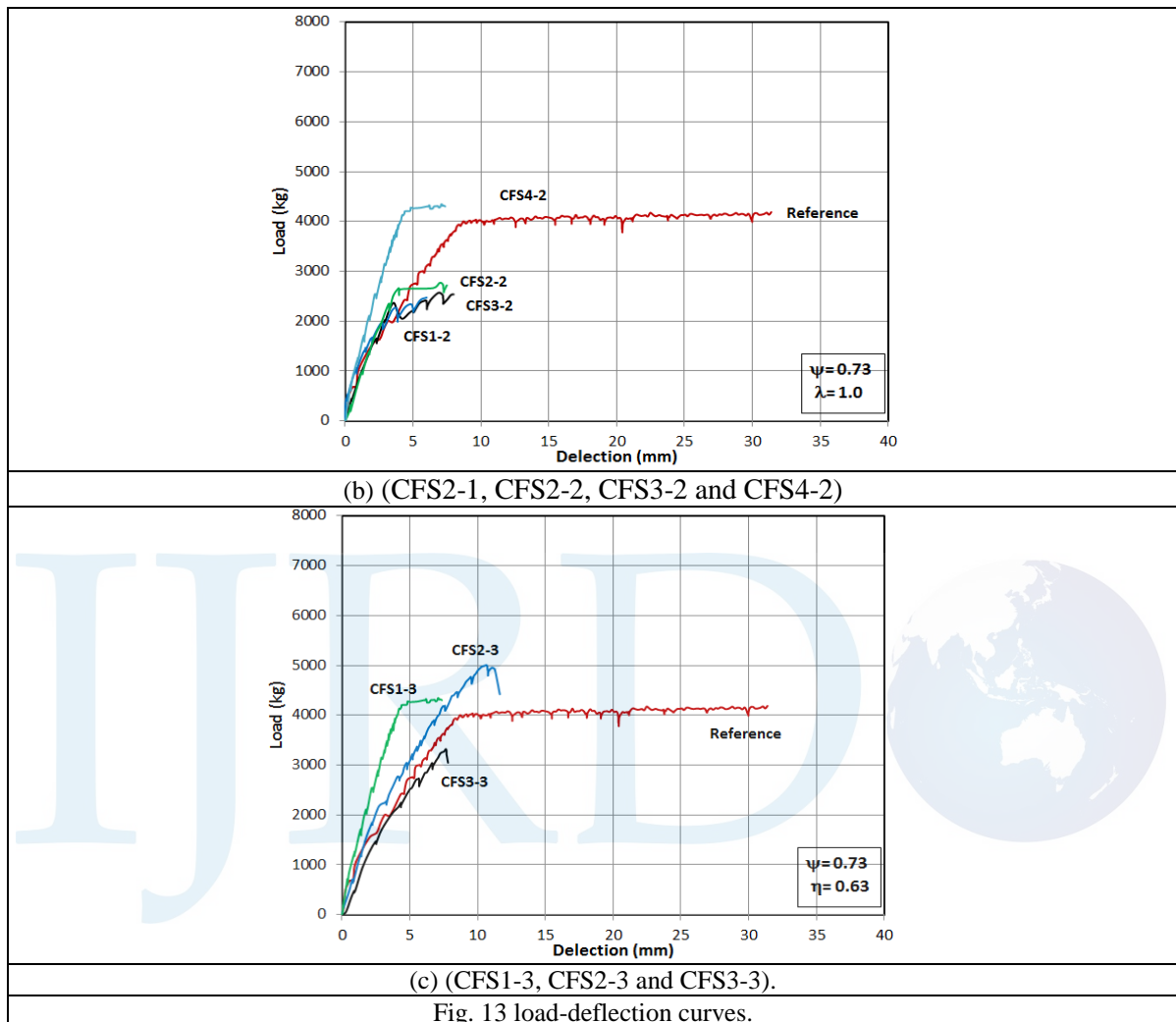


Fig. 13 load-deflection curves.

3.4 Ductility factor

Applying the concepts of fracture mechanics, with reasonable reliability there could be a safety margin against failure, and a safety margin for prediction of beam failure. Ductility factor (F_d) is expressed as the ratio of deflection at beam failure to the deflection at the concrete first crack, the ductility factor for the reference beam was 6.5, as shown in Table 3.

Figs. 14(a)-(c) shows variation of ductility factor with the normalized width, height, and length respectively. It declared that the ductility factor decreased as the beam normalized width and length increased, while variation of the normalized height had no noticeable effect on the ductility factor. The ductility factor was observed to be the highest for models (CFS3-1 and CFS3-3), highest than the reference beam, thereafter the other models record lower values for the ductility factor than the reference beam.

Table 3 Ductility factor.

Group	Specimen	Δ_{cr} (mm)	Δ_f (mm)	F_d
1	CFS1-1	2.7	7.4	2.8
	CFS2-1	3.3	17.7	5.4
	CFS3-1	4.3	33.9	7.9
2	CFS1-2	2.1	6.0	2.8
	CFS2-2	3.6	7.5	2.1
	CFS3-2	3.6	7.8	2.2
	CFS4-2	2.7	7.4	2.8
3	CFS1-3	2.7	7.4	2.8
	CFS2-3	3.5	10.6	3.1
	CFS3-3	4.3	31.2	7.2
Reference beam		4.8	31.2	6.5

Δ_{cr} : Deflection at first crack.

Δ_f : Deflection at beam failure .

F_d : Ductility factor.

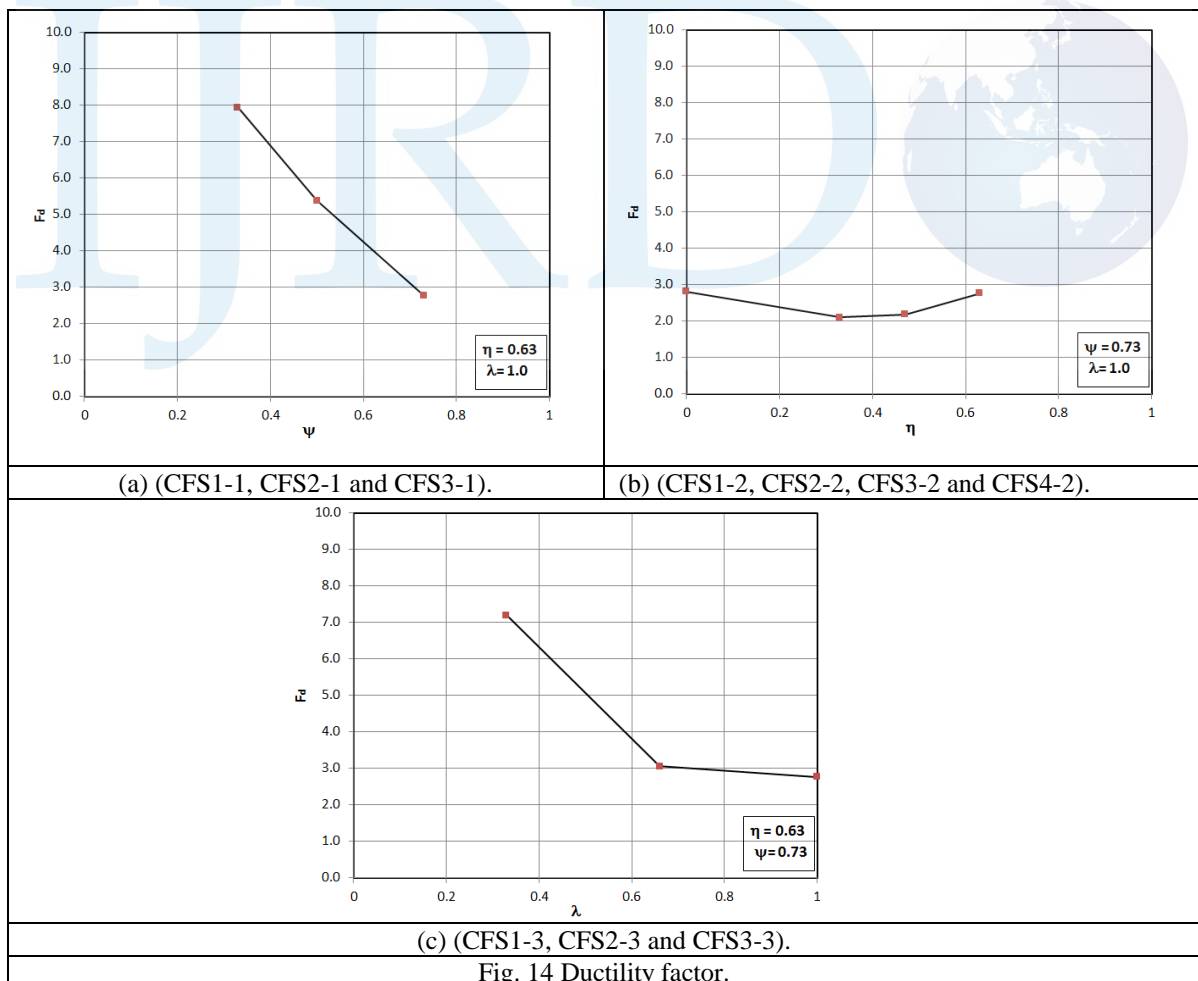


Fig. 14 Ductility factor.

CONCLUSIONS

This paper presents an experimental study on the structural performance of encased cold-formed steel (U-section) in a reinforced concrete beam. Based on the previous experimental results, the major conclusions are summarized below.

- Providing the cold-formed steel (CFS) with width less than the concrete half-width increase the beam load capacity with a significant value, also avoiding beam to fail by local buckling failure, otherwise the beam will pass through the local buckling problems.
- Concrete cracks appear early for encased beam than that of beam without cold-formed steel (CFS) for most cases.
- Using the cold-formed steel (CFS) with no web led to decreasing in the beam load capacity due to shear splitting failure.
- Using the cold-formed steel (CFS) with length less than two-thirds of beam length make good benefits of the (CFS) in increasing the beam flexure capacity than using full length, but led to brittle shear failure.
- Providing the cold-formed steel (CFS) decreases with full width and length share in decreasing the beam deflections with significant values.

References

- [1] Qiyin Shi, Bo Ma, and Aiqun Li, The Mechanical Performance Analysis of New Encased-steel Concrete, *Experimental Mechanics*, 20 (2005) 115-122
- [2] L.Fiorino. O.Iuorio. R.Landolfo, Designing CFS structures: the new school bfs in naples, *Thin-walled Structures*, 78 (2014) 37-47.
- [3] J.B.P.Lim, D.A.Nethercot, Finite element idealization of a cold-formed steel portal, *J. Struct. Eng. – ASCE*, 130 (2004) 78-94.
- [4] Wang H. and Zhang Y. Experimental and Numerical Investigation on Cold-formed Steel C-section Flexural Members, *Journal of Constructional Steel Research*, 65 (2009) 1225-1235.
- [5] Dinis, P.B. and Camotim D., Local/distortional Mode Interaction in Cold-formed Steel Lipped Channel Beams, *Thin-walled Structures*, 48 (2010) 771-785.
- [6] Pham, S.H., Pham C.H. and Hancock G.J., Direct Strength Method of Design for Shear Including Sections with Longitudinal Web Stiffeners, *Thin-Walled Structures*, 81 (2014) 19-28.
- [7] Wang, L. and Young B. Design of Cold-formed Steel Channels with Stiffened Webs Subjected to Bending, *Thin-Walled Structures*, 85 (2014) 81-92.
- [8] Ammar A., Saad N., and Wael S., Strength and Ductility of Concrete Encased Composite Beams, *Eng. and Tech. Journal* 30 (2012).
- [9] L. Krishnan, C. S. Dineshraj, S. Prema, Experimental Investigation of Cold-Formed Steel Section-Flexural Member with Triangular Web, *Journal of Mechanical and Civil Engineering*, 12 (2015) 36-39.
- [10] J. Lee, S.M.Kim, H.S.Park, Y.H.Woo, Optimum design of cold-formed steel channel beams using micro genetic algorithm, *J. Struct. Eng. – ASCE*, 27 (2005) 17-24.
- [11] W.Ma, J.Becque, I.Hajirasouliha, J.Ye, Cross-sectional optimization of cold- formed steel channels to Eurocode3, *Eng.Struct.*, 101 (2015) 641-651.
- [12] CEN, Eurocode3: Design of Steel Structures, Part1.3: General Rules — Supplementary Rules for Cold-formed Steel Members and Sheeting, in, Brussels: European Committee for Standardization (2005).
- [13] J.Z. Leng, Z.J.Li, J.K.Guest, B.W.Schafer, Shape optimization of cold-formed steel columns with fabrication and geometric end-use constraints, *Thin-Walled Structures*, 85 (2014) 271–290.